Targeted disruption of the *Hoxb-2* locus in mice interferes with expression of *Hoxb-1* and *Hoxb-4*

Jeffery R. Barrow and Mario R. Capecchi*

Howard Hughes Medical Institute, Department of Human Genetics, University of Utah, School of Medicine, Salt Lake City, Utah 84112, USA

*Author for correspondence

SUMMARY

Mice with a disruption in the *hoxb-2* locus were generated by gene targeting. 75% of the *hoxb-2* mutant homozygotes died within 24 hours of birth. While a majority of these mice had severe sternal defects that compromised their ability to breathe, some had relatively normal sternum morphology, suggesting that one or more additional factor(s) contributed to neonatal lethality. At 3-3.5 weeks of age, half of the remaining *hoxb-2* homozygotes became weak and subsequently died. All of the mutants that survived to 3 weeks of age showed marked facial paralysis similar to, but more severe than, that reported for *hoxb-1* mutant homozygotes (Goddard, J. M., Rossel, M., Manley, N. R. and Capecchi, M. R. (1996) *Development* 122, 3217-3228). As for the *hoxb-1* mutations, the facial paralysis observed in mice homozygous for the *hoxb-2* mutation results from a failure to form the somatic motor component of the VIIth (facial) nerve which controls the muscles of facial expression. Features of this phenotype closely resemble the clinical signs associated with Bell's Palsy and

Moebius Syndrome in humans. The sternal defects seen in *hoxb-2* mutant mice are similar to those previously reported for *hoxb-4* mutant mice (Ramirez-Solis, R., Zheng, H., Whiting, J., Krumlauf, R. and Bradley. A. (1993) *Cell* 73, 279-294). The above results suggest that the *hoxb-2* mutant phenotype may result in part from effects of the *hoxb-2* mutation on the expression of both *hoxb-1* and *hoxb-4*. Consistent with this proposal, we found that the *hoxb-2* mutation disrupts the expression of *hoxb-1* in *cis*. In addition, the *hoxb-2* mutation changes the expression of *hoxb-4* and the *hoxb-4* mutation, in turn, alters the pattern of *hoxb-2* expression. *Hoxb-2* and *hoxb-4* appear to function together to mediate proper closure of the ventral thoracic body wall. Failure in this closure results in severe defects of the sternum.

Key words: *Hox* genes, homeobox genes, *hoxb-1, hoxb-2, hoxb-4*, gene targeting, Moebius Syndrome, sternal development, facial nerve, mouse

INTRODUCTION

Hox genes encode transcription factors belonging to the *Antennapedia* homeodomain class. Man and mouse contain at least 39 *Hox* genes distributed on four linkage groups designated Hox A, B, C and D. This organization is believed to have arisen early in vertebrate phylogeny by quadruplication of an ancestral complex common to vertebrates and invertebrates (Pendleton et al., 1993; Holland and Garcia-Fernandez, 1996). Based on DNA sequence similarities and on the position of the genes on their respective chromosomes, individual members of the four linkage groups have been classified into 13 paralogous families. Mutational analysis in the mouse has demonstrated that these genes, alone or in concert with other *Hox* genes, are used to regionalize the embryo along its major axes (Chisaka and Capecchi, 1991; Lufkin et al., 1991; Chisaka et al., 1992; LeMouellic et al., 1992, Dollé et al., 1993; Gendron-Maguire et al., 1993; Jeannotte et al., 1993; Ramirez-Solis et al., 1993; Rijli et al., 1993; Small and Potter, 1993; Davis and Capecchi, 1994; Kostic and Capecchi, 1994; Satokata et al., 1995; Suemori et al., 1995; Boulet and Capecchi, 1996). Thus, mutations in 3′ *Hox* genes affect the

formation of anterior structures whereas disruption of 5′ genes gives rise to posterior abnormalities. Regionalization of the embryo by *Hox* genes appears to be accomplished by the controlled temporal and spatial activation of these genes such that a 3′ gene is activated prior to and in a more anterior region of the embryo than its 5′ neighbor (Duboule and Dollé, 1989; Graham et al., 1989; Duboule, 1994; Capecchi, 1997). However, *Hox* genes function as highly integrated circuits such that paralogous genes, adjacent genes on the same linkage group and even non-paralogous genes in separate linkage groups interact positively, negatively and in parallel with each other to orchestrate the morphological regionalization of the embryo (Condie and Capecchi, 1994; Rancourt et al., 1995; Davis et al., 1995; Horan et al., 1995; Davis and Capecchi, 1996; Favier et al., 1996; Fromental-Ramain et al., 1996).

In this report, we examine the effects of disrupting the *hoxb-2* gene on mouse development. The phenotype is complex, but can be understood in terms of the effect of inactivating *hoxb-2* function, combined with the consequences of disrupting the expression of two neighboring *Hox* genes, *hoxb-1* and *hoxb-4*. *Hoxb-1* and *hoxb-2* appear to function together in the specifi-

cation of the motor component of the VIIth nerve. *Hoxb-2* and *hoxb-4* are apparently both required to mediate closure of the ventral thoracic body wall. It is suggested that a failure in this closure prevents fusion of the two sternal bands and subsequent abnormal formation of the sternum.

MATERIALS AND METHODS

Targeting vector and generation of *hoxb-2⁻* mutant mice

A 12 kb DNA fragment containing the *hoxb-2* gene was isolated from an embryo-derived stem (ES) cell genomic library and was used to construct the targeting vector (Thomas and Capecchi, 1987). The fragment extended from an *Eag*I site 5′ of the *hoxb-3* gene to a *Not*I site 3′ of *hoxb-2* (Fig. 1). The KT3NP3 *neomycin resistance* cassette was inserted into the *Eag*I site in the *hoxb-2* homeobox, thus disrupting the third helix in the homeodomain of the encoded protein. KT3NP3 is a 2.7 kb *neo* cassette that is identical to the previously reported KT3NP4 (Deng et al., 1993) but lacks 400 bp from the 3′ end of the polyadenylation signal. The *hoxb-2/neo* construct was flanked by the herpes simplex virus *thymidine kinase* genes, *TK1* and *TK2*. The vector was linearized and electroporated into R1 ES cells (Nagy et al., 1993). The cells were then subjected to positive/negative selection using G418 and FIAU as previously described (Mansour et al., 1988). 77 G418/FIAU-resistant cell lines were isolated and screened for targeting events by Southern transfer analysis (Fig. 1). *Bam*HI-digested DNA from each of the cell lines was transferred to nitrocellulose and hybridized with a 500 bp *Not*I/*Bam*HI 3′ flanking probe (Fig. 1). DNA from four cell lines was found to have the expected electromobility shifts from 5.5 to 2.9 kb and each DNA sample was further analyzed with multiple restriction enzyme digests and hybridization probes in order to verify the fidelity of the homologous recombination event. Two of these cell lines, when injected into C57BL/6J blastocysts and implanted into foster mothers, gave rise to germ-line chimeras.

Genotyping of animals

Genotypic analysis was carried out on DNA extracted from tails of mice and performed either by Southern transfer analysis or by PCR amplification (Thomas et al., 1992). Southern blots were performed with the same digests and probes as described above and in Fig. 1. PCR analysis was performed using the following primers: *hoxb-2* sense primer 5′GATTGCCAGAATGCGGCGGCA3′ derived from the 5′ end of the homeobox (Rubock et al., 1990); *hoxb-2* antisense primer 5′CCCTGCGCGGCCTCGGCG3′ commencing 150 bases 3′ of the homeobox (N. Manley, unpublished sequence); RNA polymerase II (pol II) antisense primer 5′TGTTCAAGCC-CAAGCTTTCGCG3′. Briefly, the first 16 bases of the primer were derived from the 5′ end (antisense) of the RNA polymerase II promoter (bases 2-17, accession number M14101) whereas the last 6 bases were taken from the polylinker of pIC19H (*Hin*dIII, *Nru*I sites). The *hoxb-2* sense and antisense primers amplify a 359 bp fragment from wild-type template whereas a 271 bp product is amplified from the *neo* allele with the pol II and *hoxb-2* antisense primers. The PCR reactions were performed under the following cycling conditions: 95°C for 30 seconds, 60°C for 20 seconds and 72°C for 30 seconds for 35 cycles. The PCR amplified bands were resolved on 2% TreviGel500 (Trevigen) gels.

Embryos were genotyped from yolk sac DNA with the PCR primers and conditions described above. Yolk sacs were dissected from the embryos and incubated in PCR lysis buffer and proteinase K (1 mg/ml) at 50°C overnight. The yolk sac DNA samples were then boiled for 5 minutes, and an aliquot was used for PCR amplification.

RNA in situ hybridization and immunohistochemistry

RNA in situ analysis was performed with digoxigenin-labeled probes as described previously (Manley and Capecchi, 1995). The *hoxb-1* probe was a 300 bp *Pst*I/*Bam*HI fragment beginning 20 bp 3′ of the

homeobox and extending into the 3′ UTR. The *hoxb-2* probe was a 900 bp fragment isolated from a cDNA clone, containing 130 bp of 3′ coding sequences and extending into the 3′ untranslated region (Goddard et al., 1996). *The hoxb-3* in situ hybridization probe consisted of a 450 *Bam*HI/*EcoR*I fragment generated from a cDNA clone. The 5′ end of the probe is located ~330 bp downstream of the
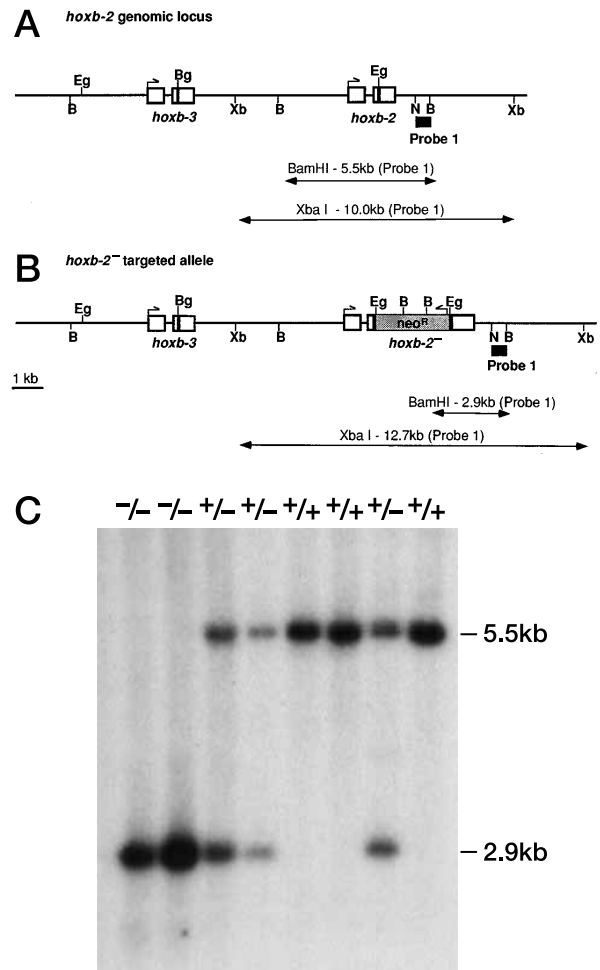

Fig. 1. Targeted disruption of the *hoxb-2* locus. (A) Map of the genomic *hoxb-2* locus. *Bam*HI- and *Xba*I-digested murine genomic DNA that was transferred to nitrocellulose and then hybridized with Probe 1 generates 5.5 kb and 10 kb bands respectively. (B) Map of the genomic *hoxb-2* locus after gene targeting. The targeting vector was constructed from a 12 kb region extending from the *Eag*I site 5′ of *hoxb-3* to a unique *Not*I site 3′ of *hoxb-2*. The *neomycin* drug resistance cassette, KT3NP3, was inserted into an *Eag*I site in the *hoxb-2* homeobox. KT3NP3 contains two *Bam*HI sites and no *Xba*I sites. Therefore, digesting DNA containing the targeted disruption with either of these enzymes will yield restriction fragments with lengths different from those of fragments from the unaltered locus. The expected band size for *Bam*HI-digested, targeted DNA is 2.9 kb while that anticipated for *Xba*I-*digested* DNA is 12.7 kb. (C) Southern blot analysis demonstrating the three *hoxb-2* genotypes. *Bam*HI-digested DNA from progeny of *hoxb-2⁻* heterozygous intercrosses was probed with the 3′ flanking probe, probe 1. Wild-type mice generate a unique 5.5 kb band, heterozygotes show the same 5.5 kb band plus a 2.9 kb band, while homozygous mutants yield only a 2.9 kb band. The probed *Xba*I digests yielded the expected bands for each of the genotypes as well (data not shown). B, *Bam*HI; Bg, *Bgl*II; Eg, *Eag*I; N, *Not*I; Xb, *Xba*I.

hoxb-3 homeobox. The *hoxb-4* probe was a 450 bp *Nae*I/*Bam*HI fragment containing the last nine *hoxb-4* codons and continuing into the 3′ untranslated sequences (Boulet and Capecchi, 1996). The *hoxa-2* probe was a 600 bp *Xho*I/*Eco*RV fragment extending from the 5′ end of the homeodomain to the end of the protein coding sequence.

Immunohistochemistry using antibodies directed against the hoxb-1 protein was carried out as described by Goddard et al. (1996). *Krox-20* immunohistochemistry was also performed as described by Goddard et al. (1996) except that the embryos were fixed in 4% paraformaldehyde. Immunodetection of neurofilament protein was performed on E10.5-E11.5 embryos with the use of the 2H3 anti-155×10^3 M_r neurofilament monoclonal antibody (Dodd et al., 1988) as described by Chisaka et al. (1992).

Histology and skeletal preparations

Newborn mice or E18.5 fetuses were asphyxiated in CO_2 and fixed in 4% formaldehyde/PBS for 24 hours or longer. The mice were then dehydrated, embedded in paraffin, sectioned and stained with hematoxylin and eosin as previously described (Mansour et al., 1993).

Skeletons were prepared as described by Chisaka and Capecchi (1991).

RESULTS

Targeted disruption of the *hoxb-2* locus

A 12 kb genomic DNA sequence encompassing the *hoxb-2* gene was used to construct the *hoxb-2* targeting vector (see Materials and Methods). A neomycin resistance cassette was inserted into the homeobox of *hoxb-2*, thereby destroying the ability of the encoded protein product to bind to specific DNA sequences (Fig. 1). The targeting vector was electroporated into R1 ES cells and positive-negative selection was used to enrich for cells containing the desired homologous recombination events (Mansour et al., 1988; Fig. 1). Four independent cell lines that carried a targeted disruption of the *hoxb-2* gene were identified. Additional restriction enzyme digests, probed with both 5′ and 3′ flanking probes, as well as an internal probe, showed that these cell lines contained no modifications other than the desired *neo* insertion into the *hoxb-2* homeobox (data not shown). Two of these cell lines were used to generate germ-line chimeras. The two colonies of mice derived from these cell lines were found to have indistinguishable phenotypes. Most of the analysis described herein involved the colony of mice derived from the 2f-4 ES cell line.

Viability and fertility of *hoxb-2* mutant mice

Mice heterozygous for the *hoxb-2 neo* mutation appeared outwardly normal and were viable and fertile. Of the mutant homozygotes, 88% died by 3-3.5 weeks of age in two stages: 75% died within 24 hours of birth, and the remaining 13% died between 21 and 25 days after birth. The eleven mutant homozygotes that survived to 3 weeks of age were readily distinguishable from their wild-type and heterozygous littermates. Most (10/11) were runted, all had narrow faces; (Fig. 2A,B) and all had receded lower lips; (Fig. 2C,D). In addition, these mutant mice had severe paralysis of the muscles of the face. They showed no movements of the whiskers and nose, did not close their eyes in response to touch and failed to move their ears in response to touch or noise. Although the facial defects closely resemble those observed in *hoxb-1* mutant homozygotes (Goddard et al., 1996), the defects in *hoxb-2* mutant mice are uniformly more severe. The narrowing of the face is first
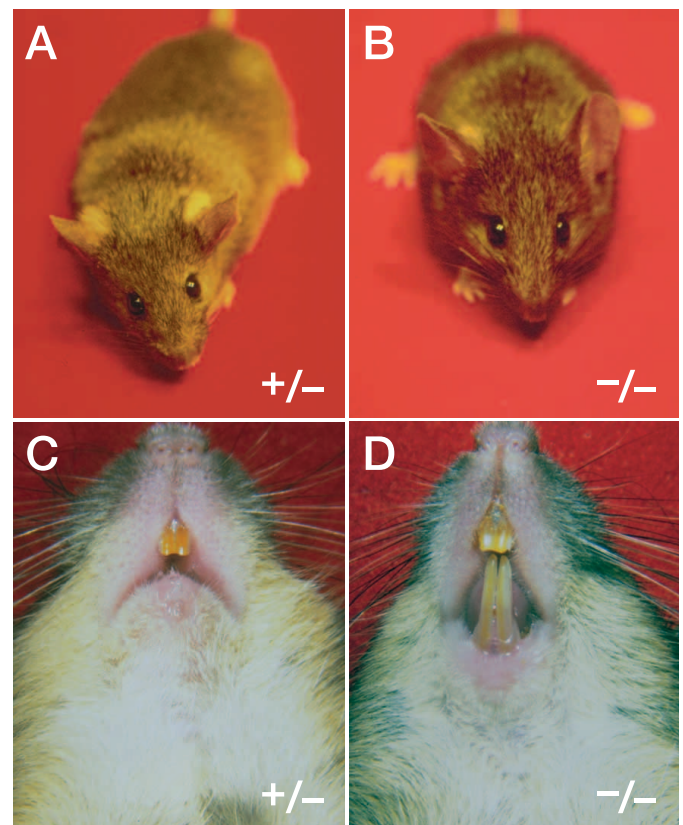

Fig. 2. External facial phenotypes of *hoxb-2⁻* mice. (A,B) Frontal view of *hoxb-2⁻* heterozygous (A) and homozygous (B) mice. The homozygous mutant has a noticeably narrower face than the heterozygote. (C,D) Ventral view of heterozygous (C) and homozygous (D) mice. The lower lip in the mutant is severely retracted compared to the control. This view also demonstrates the narrowness of the nasal (facial) region.

apparent 10 days following birth and becomes progressively more severe with age. At 3 weeks of age, approximately half of the remaining mutant homozygotes become weak and die shortly thereafter (21-25 days).

Those animals that survived past 25 days (2 males and 3 females) were fertile. However, the females had difficulty raising their litters, irrespective of the genotype of their pups. Two of the females had no surviving pups 24 hours after birth. The third lost 5/7 pups within 24 hours of birth.

As mentioned above, 75% of the *hoxb-2* mutant homozygotes died within 24 hours of birth. Genotype analysis of newborns from heterozygous intercrosses showed that the distribution of wild-type and mutant alleles did not deviate significantly from the expected Mendelian ratio (Table 1), showing that homozygous mutant animals were not dying in utero. An additional 32 mutant homozygotes derived from *hoxb-2* heterozygous or from homozygous by heterozygous intercrosses were observed within 24 hours of birth and assessed for viability. 24 of the 32 mutant homozygotes (75%) were found dead or appeared to be dying from respiratory distress. Most of the dead or dying mutants had severe sternal defects, which were readily apparent from gross examination of the newborn mice (Table 2). A smaller number appeared normal with respect to formation of the sternum, but were

Table 1. Genotypic analysis of offspring generated from
hoxb-2⁻ heterozygous intercrosses

	+/+	+/−	−/−
Weanlings (3-4 weeks)	35 (38)	80 (77)	9* (38)
Newborns	37 (34.5)	70 (69)	31 (34.5)

The newborns and weanlings represent two separate populations of mice. The figure in each column indicate the numbers for each genotypic class with the expected Mendelian ratios in parentheses.

*Two additional homozygous mutants included in results described in the text were generated by a homozygous by heterozygous intercross.

unable to nurse (i.e., did not have milk in their stomachs). Extensive facial paralysis would be expected to interfere with nursing since the orbicularis oris muscle, which surrounds the mouth, is controlled by the VIIth nerve.

Skeletal defects in _hoxb-2_ mutant homozygotes

The skeletons of 29 mutant homozygous and 39 heterozygous newborn animals were examined. Three different classes of skeletal defects were observed in the mutant homozygote.

The first class, which comprised the majority of the mutant homozygotes (24/29; 83%), had a split sternum. In spite of the high penetrance of this defect, the expressivity was variable. For example, 38% (11/29) had a severely split sternum (Fig. 3E) whereas another 34% (10/29) had a milder form of this defect in which the two sternal bands were not fused but were in closer proximity to one another (Fig. 3D). Three of the 29 showed partially fused sternums with either the top or the bottom being unfused (Fig. 3C). The five remaining newborn homozygotes had completely fused sternums; however, in one of these animals the sternebrae were not aligned properly along the ventral midline (crankshaft phenotype). None of the viable newborn mutant animals exhibited the most severe sternal abnormalities, which suggests that this defect was a major contributor to morbidity.

None of the _hoxb-2_ mutant heterozygotes had a split sternum; however, 2/39 (5%) had a crankshaft phenotype (Fig. 3B). We have never observed this defect in numerous skeletons from wild-type mice.

Very similar sternal defects were reported for mice homozygous for a targeted disruption of the first exon of the _hoxb-4_ gene (Ramirez-Solis et al., 1993). These authors reported 50% neonatal lethality and attributed all of the deaths to sternal defects. We also observed that ~50% (14/29) of the _hoxb-2_ mutant homozygotes appeared to die from severe or moderate sternal defects (Table 2) but that an additional 25% (7/29) of

Table 2. Correlation between severity of sternal defects
and viability in mutant newborns and weanlings

	Severe	Moderate	Intermediate	Mild	Normal
Dead or dying newborns	11	3	3	1	3
Living newborns	0	2	2	2	2
Survivors past 21 days	0	2*	1	1	3

*The two survivors with moderately split sternums are actually the same two reported for living newborns of the same phenotypic class. They were diagnosed as having a moderately split sternum as newborns and were returned to and raised by their respective mothers.

these mutant newborn animals died of other causes (i.e., severe facial paralysis).

In the second class of skeletal defects, _hoxb-2_ heterozygous and homozygous mice showed anterior transformations of the axis (C2) such that it more closely resembled the atlas (C1). The defect consists of a broadening of the neural arch of the axis (Fig. 4). In addition, a small number of mutants with a broadened neural arch also had an ectopic anterior arch on the ventral side of the axis, a feature normally associated only with the atlas (Fig. 4). The penetrance of the cervical vertebral transformations was 55% (16/29) in the homozygous mutants and 13% (5/39) in heterozygotes. The presence of the cervical vertebral transformations did not correlate with the presence of the sternal defects, suggesting that the two sets of abnormalities are of independent developmental origin. These cervical transformations are also observed in _hoxb-4_ mutant mice with similar penetrance (at least for the _hoxb-4ˢ_ allele; see Ramirez-Solis et al., 1993 and below). Unlike the sternal defect, the cervical vertebral transformations do not appear to compromise viability.

In the third class, both _hoxb-2_ +/− and −/− animals had a change in the orientation of the anterior arch of the atlas compared with wild-type control animals. In wild-type animals, the anterior arch protrudes ventrally, perpendicular to the vertebral column (Fig. 4). In 41% of +/− animals (16/39) and 76% of −/− animals (22/29), the anterior arch was slanted rostrally. The severity of the phenotype was more pronounced in homozygotes than it was in heterozygotes. For example, in 11/22 of the homozygous mutants possessing this defect, the anterior arch was almost parallel to the axial skeleton (data not shown) whereas in the most severe heterozygous animals, it was tilted at only a 45° angle with respect to the vertebral column (similar to that shown in Fig. 4B, which depicts a mutant homozygote). No wild-type mice appeared to have this defect. As was the case with the transformations of the cervical vertebrae, this defect was not associated with death.

Second branchial arch skeletal structures are unaffected in _hoxb-2_ mutant mice

Hoxb-2 is strongly expressed in the second branchial arch and could therefore participate in the specification of skeletal structures derived from this arch, namely the lesser horn of the hyoid, the stapes and the stylohyoid ligament. None of the 29 mutant skeletons analyzed had defects in these structures. This is in sharp contrast to mice with mutations in the other member of this paralogous family, _hoxa-2,_ in which second arch skeletal structures are not formed (Gendron-Maguire et al., 1993; Rijli et al., 1993).

Expression of hindbrain markers appears to be normal in _hoxb-2_ mutant mice

The integrity of the rhombomere pattern of the early hindbrain in _hoxb_-2 mutant homozygous embryos was examined by the analysis of the patterns of a series of molecular markers specifically expressed in the hindbrain. Mutant embryos (E8.5 and E9.5) along with heterozygous and wild-type controls were subjected to whole-mount RNA in situ hybridization analysis with _hoxa-2, hoxb-3_ or _hoxb-4_ RNA antisense probes, or to immunohistochemistry with a _krox-20_ antibody. For each gene, the boundary and level of expression in the hindbrain of _hoxb-2_ mutant homozygotes were indistinguishable from those in control embryos. This analysis showed that there were no

Table 3. Phenotypic distribution of *hox-2/hoxb-4* trans-heterozygous newborns

	Dead (dying)	Pericardial fold defect	Sternal defects intermediate to *hox-2* and *hoxb-4*	C2 to C1 transformation
Number of newborns (out of nine total)	9	3	8	7*

*Out of eight newborns total.

gross hindbrain abnormalities in these mutant embryos and that the pattern of rhombomeres (r) from r2 through r7 was normal (data not shown).

Hoxb-2 mutants have defects in the VIIth motor nucleus and VIIth nerve

Histological sections of six homozygous *hoxb-2* mutant and two heterozygous control newborn mice were examined for defects in internal structures and organs of *hoxb-2* mutant homozygous mice. In all six mutants, the VIIth motor nucleus in the pons was undetectable (Fig. 5B). This is similar to, but more extreme than, the defect seen in *hoxb-1* mutants (Goddard et al, 1996). In addition, the VIIth (facial) nerve, which consists primarily of axons from the VIIth motor nucleus, was reduced in five of the mutants (Fig. 5D,F) and not detected in the sixth (data not shown). Fig. 5D represents the mildest VIIth nerve defect, whereas the hypotrophy of the VIIth nerve shown in Fig. 5F is more typical (4/6 mutants). The facial paralysis of *hoxb-2* mutant homozygous mice, as mentioned above, can be attributed to the reduction of the motor components of the VIIth nerve, which normally control the muscles of facial expression. These defects include a retracted lower lip, a narrowed face and an inability to close the eyelids or move the whiskers and ears. Since the bones of the skull in *hoxb-2* mutant homozygotes appeared normal in size and shape, the progressive narrowing of the face with age suggests that this emaciated look results from progressive atrophy of the facial

muscles. Indeed, in a surgical examination of *hoxb-2* homozygotes at 3 weeks of age, the levator nasolabialis and levator labii maxillaris could not be detected and the remaining muscles of facial expression were reduced approximately two-fold in mass relative to control littermates (see also Goddard et al., 1996). In normal 3-week-old mice, the peripheral branches of the VIIth nerve are readily visible through a dissecting microscope following exposure by surgical dissection of the facial muscles. In *hoxb-2* mutant animals, only the zygomatic branch of the VIIth nerve could be detected and it was reduced two to three-fold in diameter.

In contrast to the VIIth nerve, the VIIth ganglion, which is largely made up of sensory nuclei, appeared to be normal in the *hoxb-2* mutant homozygotes (Fig. 5E,F). Although the VIIth ganglion shown in Fig. 5F appears somewhat smaller than the control (Fig. 5E), examination of adjacent sections showed that the ganglion is of normal size (data not shown). The fact that the VIIth ganglion is unaffected is corroborated by data obtained from immunohistochemical analyses of E10.5 and E11.5 embryos with an anti-neurofilament antibody. In *hoxb-2* mutant homozygous embryos, no difference in the
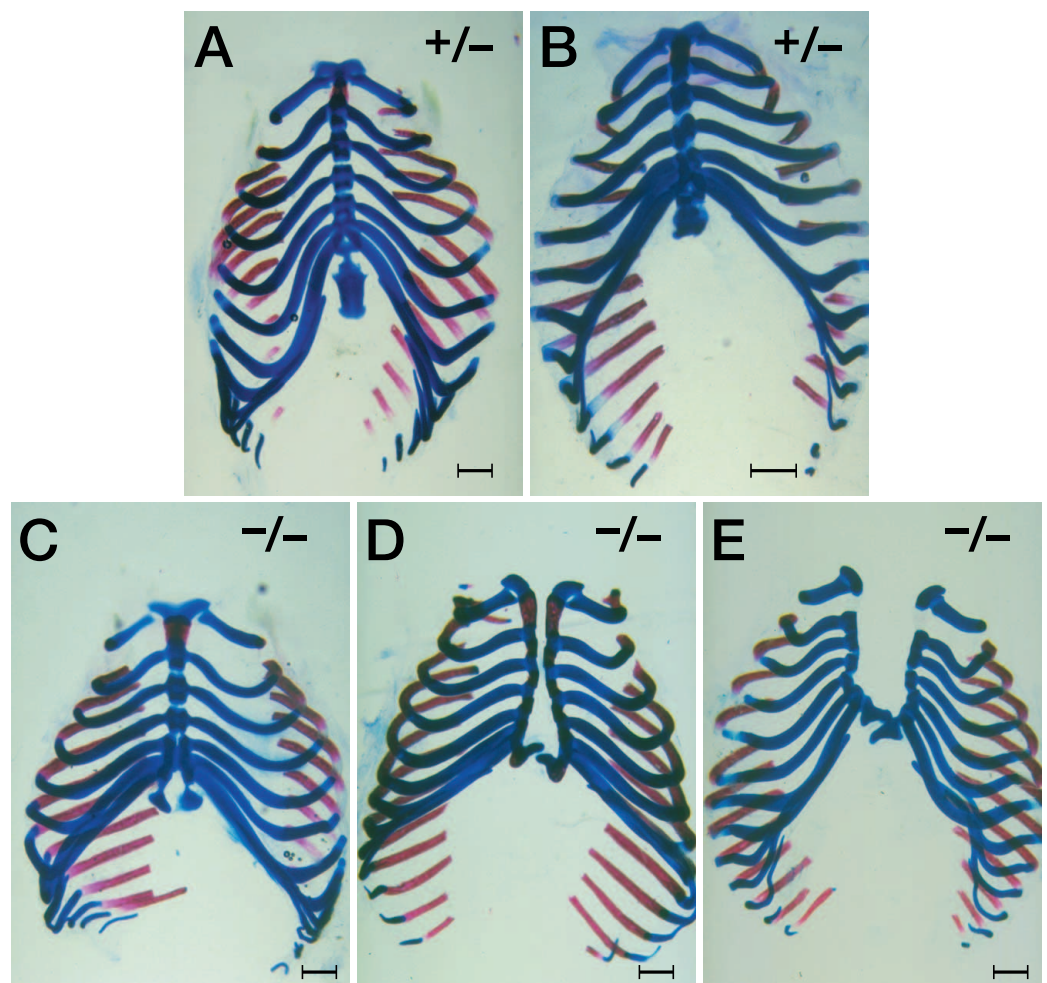

Fig. 3. Variable penetrance and expressivity of sternal defects in *hoxb-2⁻* heterozygous and homozygous newborns. (A) Normal sternum from a heterozygous control. (B) Crankshaft sternum from a *hoxb-2⁻* heterozygote showing that the sternebrae along the ventral midline are misaligned. (C) A partially split sternum of a homozygous mutant. (D) A completely split sternum from a *hoxb-2⁻* homozygote but with sternal bands in close proximity. (E) A severely split sternum from a homozygous newborn. Scale bars, 1 mm.

VIIth or other cranial ganglia was apparent (data not shown). Therefore, histological and immunohistochemical data suggest that the sensory component of the VIIth cranial nerve is not grossly affected by mutations of *hoxb-2*.

Expression of *hoxb-1* in *hoxb-2* mutants

The similarity of the facial defects in *hoxb-2* homozygous mutant mice to those observed in *hoxb-1* mutant mice (Goddard et al., 1996) suggests either that both genes have overlapping functions in specifying the motor components of the VIIth nerve, or that expression of one of the genes is altered by the mutation in the other, or both. Goddard et al. (1996) have shown that *hoxb-2* expression is normal and hoxb-1 protein is not detected in *hoxb-1* mutant homozygous embryos. Thus the facial defects in these mutants appear to be due solely to the absence of functional hoxb-1 protein. *Hoxb-1* expression in *hoxb-2* mutant embryos was examined by immunohisto-chemistry with a hoxb-1 antibody (Manley and Capecchi, 1995; Goddard et al., 1996). At E7.5 the *hoxb-2* mutant homozygous and control embryos could not be distinguished on the basis of the level and distribution of hoxb-1 protein (Fig. 6A,B). Thus, initiation of *hoxb-1* expression in the primitive streak of gastrulating embryos appears to occur normally in *hoxb-2* mutants. At E8.0 (2-4 somites), when restricted *hoxb-1* expression in rhombomere 4 is just becoming apparent, mutant and control embryos were still indistinguishable (data not shown). However, by the 6- to 9-somite stage (E8.5), clear differences in *hoxb-1* expression were apparent (Fig. 6C,D). Hoxb-1 protein was not detected in r4 of *hoxb-2* mutant homozygous embryos and expression in the caudal region of the embryo was greatly reduced. By E9.5 hoxb-1 protein was not detected anywhere in *hoxb-2* mutant homozygous embryos (Fig. 6E,F). The same results were obtained when *hoxb-1* RNA patterns were examined by in situ RNA hybridization in whole embryos, demonstrating that the effect of the *hoxb-2* mutation on *hoxb-1* expression is at the level of transcription (data not shown). The absence of hoxb-1 protein in rhombomere 4 of *hoxb-2* mutant homozygotes (i.e., from E8.5 onward) provides a molecular explanation of why *hoxb-2* mutants have facial defects similar to those of *hoxb-1* mutant mice. However, the greater severity of the facial defects in *hoxb-2* mutant homozygotes suggests that *hoxb-2* also participates in the specification of the motor component of the VIIth nerve.

The *neo* insertion in *hoxb-2* disrupts *hoxb-1* expression in *cis*

The absence of *hoxb-1* expression in *hoxb-2* mutant embryos could be due either to its being a downstream target of *hoxb-2* (regulation in *trans*) or to disruption of expression of the linked *hoxb-1* gene in *cis* by the *neo* insertion in *hoxb-2*. To distinguish between these two possibilities, *hoxb-1/hoxb-2* trans-heterozygotes were

generated and expression of the *hoxb-1* gene in the *trans*-heterozygote was determined by immunohistochemistry with the hoxb-1 antibody. If *hoxb-2* regulates *hoxb-1* in *trans*, then one would expect normal *hoxb-1* expression in the *trans*-heterozygote (Fig. 7B), whereas if the *hoxb-2 neo* insertion disrupts *hoxb-1* expression in *cis* (Fig. 7A), then hoxb-1 protein should not be synthesized (from E8.5 onward). *Hoxb-1* expression was not detected in any of the *trans*-hetrozygotes analyzed at E9.5 (Fig. 7C). Thus, it appears that the insertion of *neo* into the *hoxb-2* homeobox disrupts the expression of the linked *hoxb-1* gene in *cis*.

Phenotypic analysis corroborated the molecular results. Five adult *trans*-heterozygotes were obtained from *hoxb-1/hoxb-2* heterozygous intercrosses. None of these had sternal defects, nor did they have facial phenotypes as severe as those of the *hoxb-2* mutants, but instead had facial defects that closely resembled those observed in *hoxb-1* homozygous mutants. As a consequence of the lack of sternal defects and the milder facial defects, these *trans*-heterozygotes are viable. Therefore, as predicted, in the absence of *hoxb-1* expression, one functional copy of *hoxb-2* is sufficient for normal sternal development and ameliorating the facial defects. These results are consistent with the interpretation that *hoxb-2* functions together with *hoxb-1* in specifying the VIIth motor neurons.

hoxb-2/hoxb-4 trans-heterozygotes exhibit a split sternum and cervical transformation

As *neo* insertions into either *hoxb-2* or *hoxb-4* cause malformations of the sternum and cervical transformations in mutant
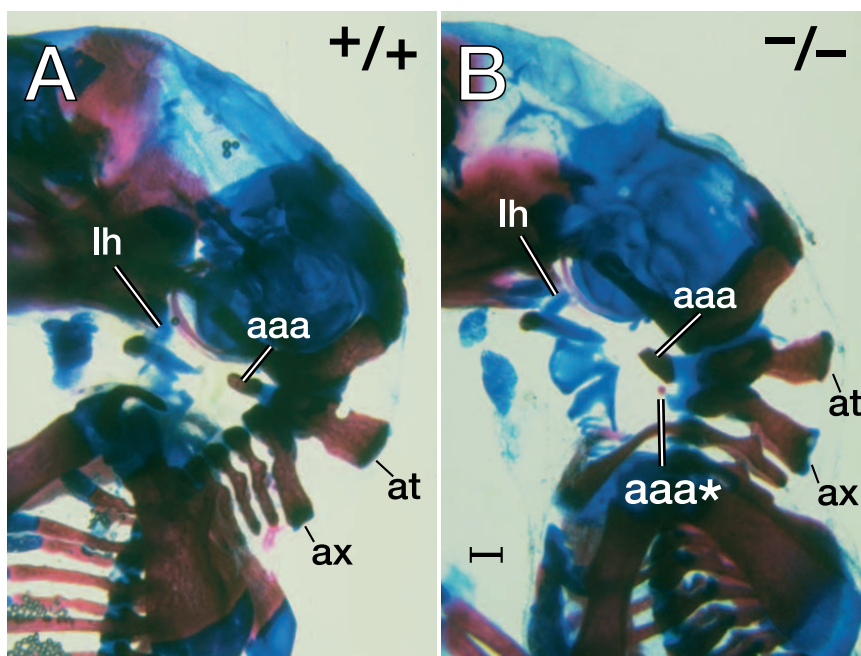

Fig. 4. Cervical abnormalities in *hoxb-2⁻* homozygous newborns. Lateral views of wild-type (A) and *hoxb-2⁻* homozygous (B) newborn skeletons. Note that, in the mutants, the anterior arch of the atlas (aaa), instead of projecting perpendicularly from the axial skeleton, slants anteriorly. In addition, the neural arch of the axis (ax) is broadened and, ventrally, there is an ectopic anterior arch (aaa*). at, atlas; ax, axis; aaa, anterior arch of the atlas; aaa*, ectopic anterior arch of the atlas; lh, lesser horn of the hyoid. Scale bar, 0.5 mm.

mice, it was important to determine the molecular basis for this overlap in phenotype. Our laboratory has generated mice with a KT3NP4 *neo* insertion in the first exon of *hoxb-4* (Manley, Barrow and Capecchi, unpublished results). Although the *neo* cassette was inserted at precisely the same *Sal*I site as in experiments reported by Ramirez-Solis et al. (1993), the sternum phenotype of our mice in a Bl/6 genetic background is completely penetrant, rather than 50% penetrant, and causes 100% lethality. The difference in phenotype in the same genetic background may reflect the use of a different *neo* cassette. The completely penetrant sternum phenotype and lethality in our mutant resembles the results reported by Ramirez-Solis et al. (1993) when their mutation was crossed into a pure *SVJ129* background. In *hoxb-2* mutant

mice, the rib cage, including the split sternum, was covered with the pericardial fold, a thin transparent membrane that aids in holding the two sternal bands together. This membrane was not present in our *hoxb-4* mutant homozygotes, so that the internal organs were exposed after removal of the skin (Manley, Barrow and Capecchi, unpublished results). Nine *hoxb-2/hoxb-4 trans*-heterozygous newborn mice were generated by intercrosses between *hoxb-2* and *hoxb-4* heterozygous mice (see Table 3). Six died at birth, the other three were in respiratory distress and were killed. The sternal defects of eight of the *trans*-heterozygotes appeared to be intermediate between those of the *hoxb-2* and *hoxb-4* mutant homozygotes. Three of the nine lacked the pericardial fold covering the gap between the two sternal bands. Eight of the newborns were processed for skeletons, and seven were found to have a transformation of the axis to atlas as seen in each of the parental mutant backgrounds. The skeletal defects in the *trans*-heterozygotes could be interpreted in two ways: (1) there is nonallelic noncomplementation between the two genes (i.e. the genes have overlapping function, or the gene products function in a common complex) and/or (2) the expression of one (or both) of the genes is altered in the other mutant background.

hoxb-4 is not expressed in the ventral body wall of *hoxb-2* mutant homozygous embryos

To determine whether *hoxb-4* was expressed normally in *hoxb-2* mutant homozygotes, whole-mount *hoxb-4* RNA in situ hybridization analysis was carried out on E9.5 and E12.5 *hoxb-2* mutant and control embryos. At E9.5 no differences in *hoxb-4* expression were seen between mutant and control embryos (data not shown). However, a significant change in the pattern of *hoxb-4* expression in *hoxb-2* mutants relative to controls was observed at E12.5. The *hoxb-4* hybridization signal observed in cells extending from the neural tube to the ventral body wall in normal embryos (Fig. 8A-D) was absent in *hoxb-2⁻* homozygotes (Fig. 8E,F). It is not certain whether this change in expression contributes to the sternal defects observed in *hoxb-*
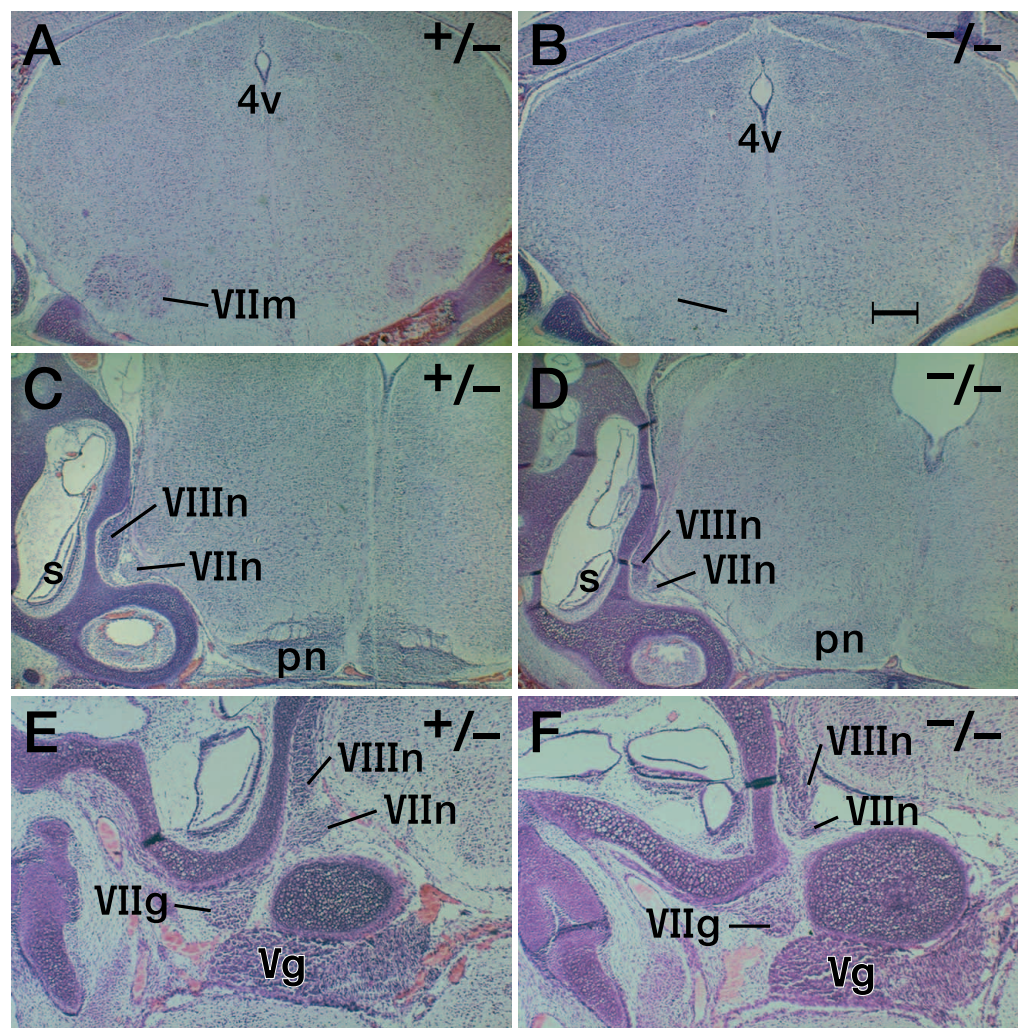

Fig. 5. Defects in the motor components of the VIIth (facial) cranial nerve of *hoxb-2⁻* homozygous animals. Transverse 10 μm paraffin sections taken from the pons region of heterozygous (A,C,E) and homozygous (B,D,F) newborns. The sections were stained with hematoxylin and eosin. (A,B) Sections demonstrating the presence (A) and absence (B) of the VIIth motor nucleus (VIIm) in a *hoxb-2⁻* heterozygote and homozygote, respectively. The indicator in B shows the general area where the VIIth motor nucleus should be located. (C-F) Sections showing the decrease in size of the VIIth nerve (VIIn) in *hoxb-2⁻* homozygotes (D,F) relative to heterozygous controls (C,E). The mutant in F had a greater reduction in the nerve than the homozygote in D. E and F also compare the size and structure of the VIIth ganglion (VIIg). Serial sections show the two ganglia to be virtually the same. 4v, fourth ventrical; pn, pontine nucleus; s, saccule; Vg, Vth ganglion; VIIg, VIIth ganglion; VIIm, VIIth motor nucleus; VIIn, VIIth nerve; VIIIn, VIIIth nerve. Scale bar, 300 μm in A-D, 170 μm in E-F.

2 mutant homozygous mice. However, our *hoxb-4* mutant mice showed an embryonic phenotype not reported by Ramirez-Solis et al. (1993). Homozygous *hoxb-4* mutant embryos at E13.5 and later, showed a failure of ventral body wall closure. This failure could underlie the formation of a split sternum in *hoxb-2* and *hoxb-4* mutant mice (Manley, Barrow and Capecchi, unpublished results). That is, closure of the ventral body wall may be a necessary prerequisite for bringing together the two separate sternal bands, which then allows proper fusion to occur. Thus, the lack of *hoxb-4* expression in the ventral body wall in *hoxb-2* mutant embryos could well contribute to the sternal defects observed in these mutant mice. In addition, we found an overall decrease in the levels of *hoxb-*

4 expression in the cervical prevertebrae that could contribute to the cervical transformations in *hoxb-2* mutant homozygotes.

As was the case with *hoxb-1* and *hoxb-2*, it is important to determine whether the changes in *hoxb-4* expression in the *hoxb-2* mutant homozygotes are due to an effect of the *hoxb-2* mutation in *cis* or if *hoxb-4* is a downstream target of *hoxb-2* (i.e., a *trans* effect). Unfortunately, a *cis/trans* test which uses *hoxb-2/hoxb-4* *trans*-heterozygotes cannot be carried out by the use of RNA in situ hybridization, because *hoxb-4* mutant homozygotes generate abortive transcripts initiated from within the *neomycin resistance* gene that interfere with this analysis. We are currently trying to generate a hoxb-4 antibody, which will permit this analysis.

hoxb-2 is down regulated in rhombomere 6 in *hoxb-4* mutant embryos

Since the sternal defects seen in *hoxb-4* mutants could be due in part to disrupted expression of *hoxb-2*, it was also important to determine whether *hoxb-2* expression is normal in a *hoxb-4* mutant background. RNA in situ hybridization analysis uncovered a subtle but reproducible difference of *hoxb-2* expression between *hoxb-4* mutants and control embryos at E9.5 (Figs. 9A-C). In normal embryos, *hoxb-2* is expressed strongly in r3-r5, slightly reduced in r6 and then at a basal level in the rest of the neural tube (Sham et al., 1993; and this work, Fig. 9A). In addition, it is expressed in neural crest emanating from r4 and to a lesser extent in neural crest cells migrating from r6 (Fig. 9A). In *hoxb-4* mutant homozygotes, the *hoxb-2* expression pattern was similar to controls except that, in r6, the level of expression was reproducibly lowered. In addition, we were not able to detect *hoxb-2* expression in neural crest cells emanating from r6 (Figs 9B,C). Expression of *hoxb-2* in *hoxb-4* mutant homozygous embryos was also examined at E12.5 but no difference in expression pattern relative to control embryos was apparent.

Hoxb-2 expression was also examined in *hoxb-2/hoxb-4* *trans*-heterozygotes in order to determine whether the changes in *hoxb-2* expression in the *hoxb-4* mutant embryos were due to a *cis* or *trans* effect. The same changes in *hoxb-2* expression that were observed in the *hoxb-4* mutant homozygous embryos were observed in the *hoxb-2/hoxb-4* *trans*-heterozygous embryos (Fig. 9B-D), demonstrating that the *hoxb-4* mutation affects *hoxb-2* expression in *cis*.
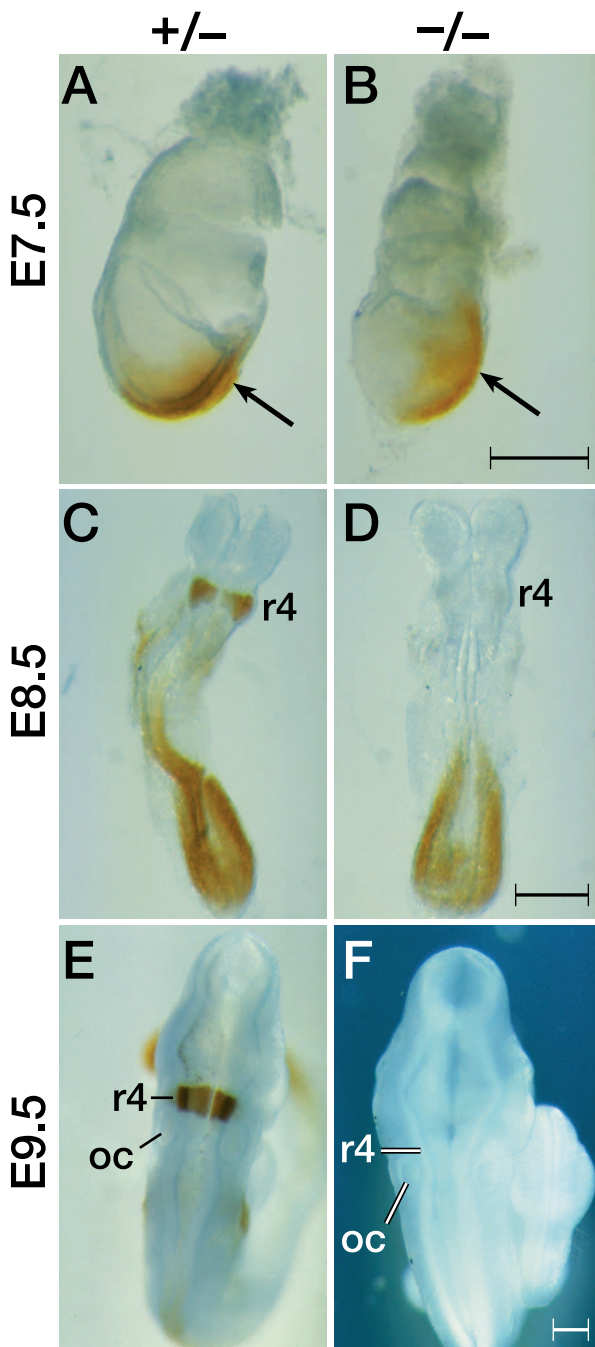

Fig. 6. Comparison of *hoxb-1* expression in *hoxb-2⁻* heterozygous (A,C,E) and homozygous (B,D,F) embryos. (A,B) Lateral views of E7.5 embryos subjected to immunohistochemistry with a hoxb-1-specific antibody. *Hoxb-1* expression in the embryos appears in the primitive streak (arrows), neurectoderm, node and mesoderm. The variability in staining between A and B is due to age differences*. (C,D) Dorsal views of E8.5 (6-9 somites) *hoxb-2⁻* heterozygous and homozygous embryos. The heterozygous embryo (C) has marked staining in rhombomere 4 (r4) and in the caudal region (lateral and presomitic mesoderm, and primitive streak). In contrast, the mutant has no *hoxb-1* expression in r4 and lighter staining more caudally. (E,F) Dorsal views of E9.5 embryos. The heterozygous embryo (E) shows intense staining in r4 and in the tail bud. (F) The *hoxb-2⁻* mutant embryo shows no *hoxb-1* expression in r4 or in the tail. r4, rhombomere 4; oc, otocyst. Scale bars, 300 μm. *E7.5 embryos demonstrated enormous variability with respect to hoxb-1 expression; however, these changes correlated to the relative age not the genotype of the embryos.
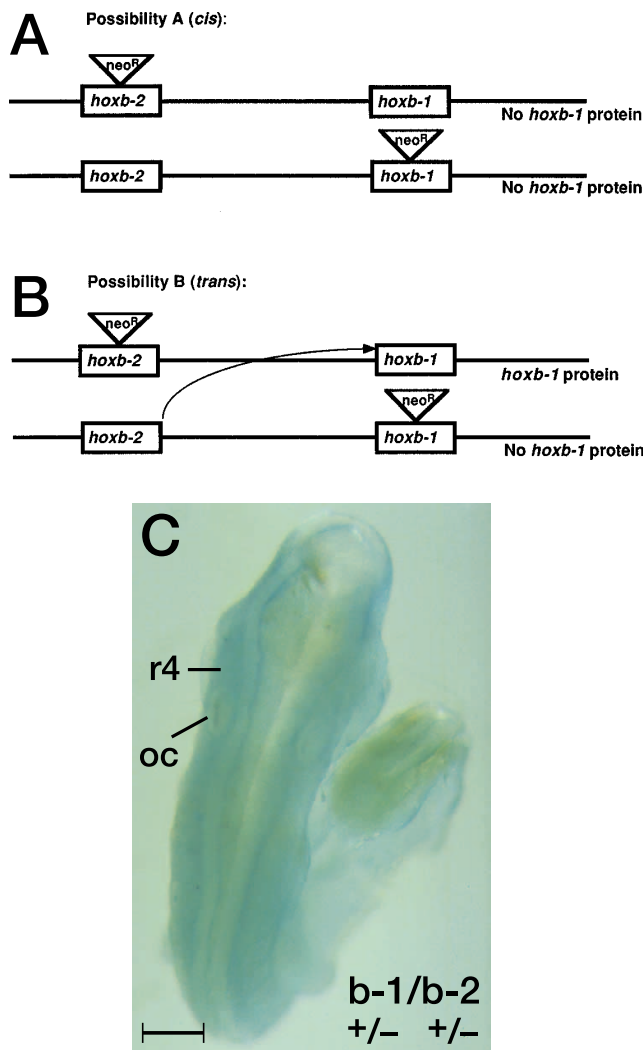
Fig. 7. Determination of the *cis* or *trans* nature of mutant *hoxb-2* influences on *hoxb-1* expression. (A,B) Schematic diagrams representing the 3′ region of the hox B locus in *hoxb-2⁻/hoxb-1^neoB* *trans*-heterozygous embryos. (A) Possibility A states that, if the *neo* insertion in the *hoxb-2* gene is disrupting expression of the linked *hoxb-1* gene (*cis*), then synthesis of hoxb-1 protein in *trans*-heterozygous embryos will not be possible. (B) Possibility B predicts that if *hoxb-1* is a downstream target of *hoxb-2,* then the former will be expressed in *trans*-heterozygous embryos because functional hoxb-2 protein will be capable of activating *hoxb-1* in *trans*. (C) Dorsal view of an E9.5 *hoxb-1/hoxb-2 trans*-heterozygote subjected to immunohistochemistry with the *hoxb-1*-specific antibody. There is no staining in rhombomere 4 (r4). oc, otocyst. Scale bar, 300 μm.

DISCUSSION

Hoxb-2 mutant homozygotes have a complex phenotype that includes atrophy and paralysis of the facial muscles of expression, defects in the formation of the sternum and transformations of cervical vertebrae. The facial defects are similar to the clinical profile of humans born with Moebius Syndrome (Moebius, 1888). Both the human and mouse disorders are associated with a failure to form the motor component of the VIIth (facial) nerve. The facial defects common to *hoxb-2* mutant homozygotes are also very similar to, but more severe
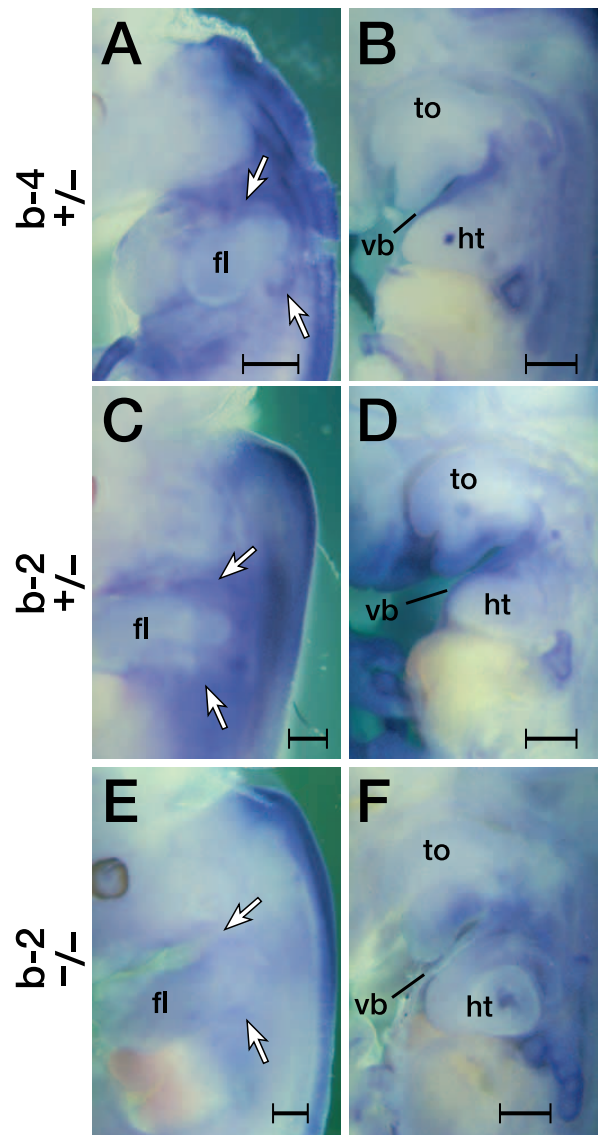

Fig. 8. Altered expression of *hoxb-4* in a *hoxb-2⁻* background. (A,C,E) External lateral views of E12.5 hemisected embryos subjected to RNA in situ hybridization with a *hoxb-4* antisense probe. (B,D,F) Internal lateral views of similarly treated embryos. *Hoxb-4* and *hoxb-2* heterozygous embryos (A,C, respectively) show expression of *hoxb-4* in a region extending from the neural tube, over and under (arrows) the forelimb (fl) and extending to the ventral body wall. (E) The *hoxb-2* homozygous mutant expresses *hoxb-4* in the neural tube but no transcripts can be detected on either side (arrows) of the forelimb (fl) nor in the ventral body wall. (B,D) *Hoxb-4* transcripts are found in the ventral body wall (vb) of *hoxb-4* and *hoxb-2* heterozygous embryos, respectively. (F) No *hoxb-4* expression is detected in the ventral body wall (vb) of the *hoxb-2* homozygous mutant. fl, forelimb; ht, heart; to, tongue; vb, ventral body wall. Scale bars, 500 μm.

than, those seen in *hoxb-1* mutant mice (Goddard et al., 1996). In one of the *hoxb-1* mutant alleles that we generated, *hoxb-1^neoB,* the coding sequences in both the first and second exons were disrupted. This mutant allele, therefore, is likely to represent a null mutation. However, since *hoxb-2* mutant homozygotes show a more severe facial phenotype than *hoxb-*

1^{neoB} homozygotes, it is likely that the loss of hoxb-2 protein contributes directly to the facial defects, above and beyond the effect of the *neo* insertion in the *hoxb-2* gene on *hoxb-1* expression.

The co-participation of *hoxb-2* with *hoxb-1* in specifying the formation of the motor component of the VIIth nerve is apparent from three perspectives. Particular features of the phenotype, such as the narrowness of the face, the receding lower lip, or the level of lethality at birth, that are attributable to deficiences of the VIIth nerve, are all more pronounced in *hoxb-2* than in *hoxb-1* mutants. A second argument suggesting direct interactions between *hoxb-1* and *hoxb-2* in specifying the motor component of the VIIth nerve centers around the phenotype of *hoxb-1/hoxb-2 trans*-heterozygotes. These mice, in effect, have no functional

copies of the *hoxb-1* gene, but one functional copy of the *hoxb-2* gene. These mice, as predicted if there is a direct contribution of *hoxb-2* to the formation of the VIIth nerve, have less severe facial defects than those in *hoxb-2* mutant homozygotes (which have no functional copies of either the *hoxb-1* or *hoxb-2* genes). Third, the variability in the expressivity of the facial defects is greater in *hoxb-1* than in *hoxb-2* mutant mice. For example, in *hoxb-1* mutant homozygotes, it is not uncommon to observe complete paralysis in the facial muscles on one side of the face, but only mild paralysis on the contralateral side. In *hoxb-2* mutant homozygotes, uniform paralysis of both sides of the face is observed. Variability of expressivity of a mutant phenotype often suggests stochastic compensation for the mutant gene product by another gene product. Conversely, reduction in the variability of expressivity suggests reduced capacity for this type of compensation. If *hoxb-1* and *hoxb-2* compensate for each other in specifying the VIIth nerve then, in the absence of both gene functions, we would anticipate reduction in the variability of expressivity in this defect.

Although *hoxb-2* mutant homozygous mice show less variability in the expressivity of the facial defects relative to *hoxb-1* mutants, they nevertheless still show some variability in this phenotype. For example, *hoxb-2* mutant homozygotes show three classes of viability attributable to VIIth nerve defects: those that die within 24 hours of birth with normal sternums, those that die between 21 and 25 days of age, and those that have a normal lifespan. This variability in expressivity is probably due to compensation by yet a third *Hox* gene, *hoxa-1*. Indeed, mice doubly mutant for *hoxa-1* and *hoxb-1* show severe exacerbation of the *hoxb-1* mutant phenotype (Rossel and Capecchi, unpublished results). Thus, at least three *Hox* genes appear to participate in the specification of the motor component of the VIIth nerve, *hoxb-1*, *hoxb-2* and *hoxa-1*.

Besides its apparent direct involvement in VIIth nerve formation, the *hoxb-2* mutation clearly disrupts expression of *hoxb-1*. Interestingly, *hoxb-1* transcription and protein synthesis in the primitive streak of the gastrulating mouse embryo appears to be initiated normally in *hoxb-2* mutants. However, the sustained, high level of *hoxb-1* expression in rhombomere 4 is eliminated. This was an unexpected result because Marshall et al. (1994), have demonstrated that *cis* regulatory elements in close proximity to the *hoxb-1* gene were sufficient to recapitulate normal *hoxb-1* r4 expression in transgenic mice. Further, this expression was sensitive to autoregulation (Pöpperl et al., 1995). The *hoxb-2* mutation is ~15 kb from the 5′ end of *hoxb-1*, yet it is capable of eliminating *hoxb-1* r4-specific expression. *Cis/trans* analysis with the use of *hoxb-1/hoxb-2-trans*-heterozygotes, showed that the *hoxb-2* mutation affects *hoxb-1* expression in *cis*. It has not been determined whether the *neo* insertion into the *hoxb-2* homeobox directly disrupts a critical *hoxb-1 cis* regulatory element, or whether the *neo* gene itself interferes with *hoxb-1* expression. We may be able to distinguish between these two possibilities by generating a new *hoxb-2* mutant allele, in which the *neo* gene is flanked by bacteriophage loxP/CRE recognition sites, to allow removal of the *neo* gene with CRE recombinase (Gu et al., 1993). In either case, the above results highlight the complexity of the regulatory networks used to control *Hox* gene expression within the complex and emphasize the possibility that mutations distal to a gene can have profound effects on its expression. Indeed, the interspersal and sharing of *cis* regulatory elements among *Hox*
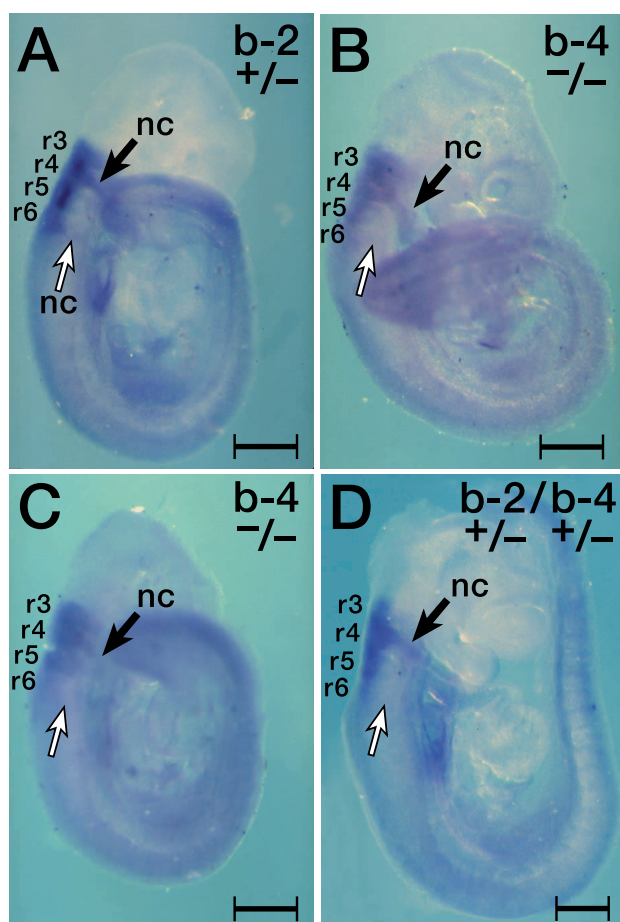

Fig. 9. Abnormal *hoxb-2* expression in *hoxb-4* mutants. (A-D) Lateral views of E9.5 embryos subjected to RNA in situ hybridization using an antisense *hoxb-2* probe. (A) Expression of *hoxb-2* in a *hoxb-2⁻* heterozygous control. Strong expression is seen in rhombomeres 3-5 (r3-5) and to a lesser extent in r6. A basal level of staining is seen in the rest of the neural tube. In addition, *hoxb-2* expression is seen in neural crest (nc) migrating from r4 (closed arrow) and r6 (open arrow). (B,C) *Hoxb-4* −/− embryos show only basal levels of *hoxb-2* expression in r6. In addition, neural crest migrating from r6 is not expressing *hoxb-2*. (D) The *hoxb-2/hoxb-4 trans*-heterozygote has a *hoxb-2* expression pattern indistinguishable from the *hoxb-4* −/− embryos suggesting that the *neo* insertion in *hoxb-4* affects *hoxb-2* expression in *cis* (Fig. 7A,B). Scale bars, 300 μm.

genes in the same linkage group may be a major constraint to the dispersal of *Hox* genes from their respective linkage groups during evolution (van der Hoeven et al., 1996).

Hoxb-2 mutant homozygotes are also characterized by severe defects in the formation of the sternum and by apparent homeotic transformations of the second cervical vertebra towards the identity of C1. Both of these defects are also seen in *hoxb-4* mutant homozygotes (Ramirez-Solis et al., 1993). Ramirez-Solis et al. (1993) generated two mutant alleles of *hoxb-4*, one containing a *neo* insertion in the first exon, the second with a frameshift mutation in the second exon, which encodes the homeodomain. Only mice homozygous for the *neo* insertion in the first exon showed defects in the formation of the sternum. The two sternal bands are produced in these mutant mice, but they fail to come together and fuse. We have also generated mice with a *neo* insertion in the first exon of *hoxb-4* (Manley, Barrow and Capecchi, unpublished results). The sternum defects in these mutant mice are similar to those reported by Ramirez-Solis et al. (1993) except that they are more severe (i.e., these mutant mice show 100% rather than 50% penetrance of the sternal defects in a BL/6 genetic background) such that all of the homozygous mutant neonates die within 24 hours of birth. We have noted that these mutant mice have defects in ventral body wall closure. It is reasonable to suggest that a failure in ventral body wall closure would prevent the two sternal bands from coming together and fusing. Interestingly, *hoxb-4* is expressed during embryogenesis in ventral body wall cells that are presumed to contribute to the pericardial fold used for closure. In *hoxb-2* mutant mice, this component of *hoxb-4* expression is disrupted. Reciprocally, the *neo* insertion in the first exon of *hoxb-4* appears to eliminate *hoxb-2* expression in neural crest cells emanating from rhombomere 6. In the chick, neural crest cells from r6-r8 contribute to the pericardial fold used for ventral body wall closure (Männer et al., 1995; Waldo et al., 1996). Based on these observations, we propose as a working model that the sternal defects observed in *hoxb-2* and *hoxb-4* mutant mice are secondary to the defects in ventral body wall closure and that both *hoxb-2* and *hoxb-4* are required for this morphogenetic process. Thus, only mutations that affect the expression of both *hoxb-2* and *hoxb-4* show defects in ventral body wall closure and sternum formation. For example, mice with a frameshift mutation in the second exon of *hoxb-4*, which certainly compromises the ability of the hoxb-4 protein to bind to specific DNA sequences, do not have sternum defects (Ramirez-Solis et al., 1993). It is presumed that *hoxb-2* expression is not affected in these mutant mice. On the contrary, mice homozygous for either the *hoxb-2* mutation or the *hoxb-4* mutation (*neo* insertion in the first exon) or mice *trans*-heterozygous for the *hoxb-2* and *hoxb-4* mutation have problems with ventral body wall closure and sternum defects. In these three latter genotypes, expression of both *hoxb-2* and *hoxb-4* was shown to be compromised. Since mice with *hoxb-4* mutations that only affect hoxb-4 protein function do not have defects in the formation of the sternum, it could be argued that only *hoxb-2* is critical for this function. However, this does not appear to be the case since *hoxb-4* mutations that do affect the function of both *hoxb-2* and *hoxb-4* have more severe sternum defects than mice with the *hoxb-2* mutation.

The transformation of the second cervical vertebra (axis) to a form resembling the first cervical vertebra (atlas) is similar in *hoxb-2* mutant mice and in mice homozygous for either of the *hoxb-4* mutant alleles (Ramirez-Solis et al., 1993, and herein).

The penetrance of this defect is also similar in *hoxb-2* and *hoxb-4* genotypes. We interpret these results to indicate that the C2 cervical transformation is primarily caused by a loss of *hoxb-4* function. Consistent with this interpretation, a general reduction in *hoxb-4* expression is observed in the prevertebrae of *hoxb-2* mutant embryos relative to normal controls.

Hoxb-3 is located between *hoxb-2* and *hoxb-4* on the mouse chromosome. It is curious that the *hoxb-2* mutation was found to affect the expression of *hoxb-4* but not *hoxb-3*. The selective effects of the *hoxb-2* mutation on neighboring *Hox* gene expression again emphasizes the intricacies in the distribution of the regulatory elements controlling neighboring *Hox* genes.

A majority of the defects observed in *hoxb-2* mutant mice can be attributed to a combination of alteration in the expression of neighboring *Hox* genes, *hoxb-1* or *hoxb-4*, and the loss of *hoxb-2* function. However, there are two defects seen in *hoxb-2* mutant mice not observed in either *hoxb-1* or *hoxb-4* mutant mice. First, *hoxb-2* homozygous females show a marked loss of ability to raise pups regardless of the pups' genotype. The cause of this defect is not known. Second, the orientation of the anterior arch of the atlas relative to the vertebral column is altered in *hoxb-2* mutant homozygotes. These phenotypes thus seem to arise directly from the loss of *hoxb-2* function.

Surprisingly, the *hoxb-2* mutant phenotype does not overlap significantly with the *hoxa-2* phenotype (Gendron-Maguire et al., 1993; Rijli et al., 1993). Specifically, *hoxb-2* mutant homozygotes do not have defects in skeletal elements derived from the second branchial arch. This situation is similar to what is observed in mice individually mutant for *hoxa-3* and *hoxd-3* (Chisaka and Capecchi, 1991; Condie and Capecchi, 1993). Although mice homozygous for mutations in these individual genes did not share overlapping phenotypes, double mutant mice showed exacerbation of both *hoxa-3* and *hoxd-3* defects (Condie and Capecchi, 1994). Thus, although these two genes individually have separate functions, in the double mutants it is apparent that they also strongly interact. We anticipate that similar interactions between *hoxa-2* and *hoxb-2* will be evident in *hoxa-2, hoxb-2* double mutants.

In summary, *hoxb-2* mutant homozygous mice with a *neo* insertion in the homeobox have a complex phenotype. The complexity of the phenotype results, to a large extent, from alterations in subdomains of the *hoxb-1* and *hoxb-4* expression patterns. However, *hoxb-2* itself also appears to be a participant with *hoxb-1* and *hoxb-4* in specification of the motor component of the VIIth nerve and in the formation of an intact sternum, respectively. Ironically, this participation would not have surfaced if the *hoxb-2* mutation had not concomitantly disrupted the expression of neighboring *Hox* genes as well as its own function.

REFERENCES

Boulet, A. M. and Capecchi, M. R. (1996). Targeted disruption of *hoxc-4* causes esophageal defects and vertebral transformations. *Dev. Biol.* **177**, 232-249.

Capecchi, M. R. (1997). The role of *Hox* genes in hindbrain development. In *Molecular and Cellular Aspects of Neural Development*(ed. W. M. Cowan, T. M. Jessell and S. L. Zipursky) pp. New York: Oxford University Press. (In press).

Chisaka, O. and Capecchi, M. R. (1991). Regionally restricted developmental defects resulting from targeted disruption of the mouse homeobox gene *hox-1.5. Nature* **350**, 473-479.

Chisaka, O., Musci, T. S. and Capecchi, M. R. (1992). Developmental defects of the ear, cranial nerves and hindbrain resulting from targeted disruption of the mouse homeobox gene *Hox-1.6. Nature* **355**, 516-520.

Condie, B. G. and Capecchi, M. R. (1993). Mice homozygous for a targeted disruption of *Hoxd-3* (*Hox-4.1*) exhibit anterior transformations of the first and second cervical vertebrae, the atlas and the axis. *Development* **119**, 579-595.

Condie, B. G. and Capecchi, M. R. (1994). Mice with targeted disruptions in the paralogous genes *hoxa-3* and *hoxd-3* reveal synergistic interactions. *Nature* **370**, 304-307.

Davis, A. P. and Capecchi, M. R. (1994). Axial homeosis and appendicular skeleton defects in mice with a targeted disruption of *hoxd-11. Development* **120**, 2187-2198.

Davis, A. P. and Capecchi, M. R. (1996). A mutational analysis of the 5′ Hox D genes: Dissection of genetic interactions during limb development in the mouse. *Development* **122**, 1175-1185.

Davis, A. P., Witte, D. P., Hsieh-Li, H. M., Potter, S. S. and Capecchi, M. R. (1995). Absence of radius and ulna in mice lacking *hoxa-11* and *hoxd-11. Nature* **375**, 791-795.

Deng, C., Thomas, K. R. and Capecchi, M. R. (1993). Location of crossovers during gene targeting with insertion and replacement vectors. *Mol. Cell. Biol.* **13**, 2134-2140.

Dodd, J., Morton, S. B., Karagogeos, D., Yamamoto, M. and Jessell, T. M. (1988). Spatial regulation of axonal glycoprotein expression on subsets of embryonic spinal neurons. *Neuron* **1**, 105-116.

Dollé, P., Dierich, A., LeMeur, M., Schimmang, T., Schuhbaur, B., Chambon, P. and Duboule, D. (1993). Disruption of the *Hoxd-13* gene induces localized heterochrony leading to mice with neotenic limbs. *Cell* **75**, 431-441.

Duboule, D. (1994). Temporal colinearity and the phylotypic progression: a basis for the stability of a vertebrate Bauplan and the evolution of morphologies through heterochrony. *Development* **1994 Supplement**, 135-142.

Duboule, D. and Dollé, P. (1989). The structural and functional organization of the murine *Hox* gene family resembles that of *Drosophila* homeotic genes. *EMBO J.* **8**, 1497-1505.

Favier, B., Rijli, F. M., Fromental-Ramain, C., Fraulob, V., Chambon, P. and Dollé, P. (1996). Functional cooperation between the non-paralogous genes *Hoxa-10* and *Hoxd-11* in the developing forelimb and axial skeleton. *Development* **122**, 449-460.

Fromental-Ramain, C., Warot, X., Lakkaraju, S., Favier, B., Haack, H., Birling, C., Dierich, A., Dollé, P. and Chambon, P. (1996). Specific and redundant functions of the paralogous *Hoxa-9* and *Hoxd-9* genes in forelimb and axial skeleton patterning. *Development* **122**, 461-472.

Gendron-Maguire, M., Mallo, M., Zhang, M. and Gridley, T. (1993). *Hoxa-2* mutant mice exhibit homeotic transformation of skeletal elements derived from cranial neural crest. *Cell* **75**, 1317-1331.

Goddard, J. M., Rossel, M., Manley, N. R. and Capecchi, M. R. (1996). Mice with targeted disruption of *hoxb-1* fail to specify VIIth nerve motoneurons. *Development* **122**, 3217-3228.

Graham, A., Papalopulu, N. and Krumlauf, R. (1989). The murine and *Drosophila* homeobox gene complexes have common features of organization and expression. *Cell* **57**, 367-378.

Gu, H., Zou, Y.-R. and Rajewsky, K. (1993). Independent control of immunoglobulin switch recombination at individual switch regions evidenced through Cre-*loxP*-mediated gene targeting. *Cell* **73**, 1155-1164.

Holland, P. W. H. and Garcia-Fernandez, J. (1996). *Hox* genes and chordate evolution. *Dev. Biol.* **173**, 382-395.

Horan, G. S. B., Ramírez-Solis, R., Featherstone, M. S., Wolgemuth, D. J., Bradley, A. and Behringer, R. R. (1995). Compound mutants for the paralogous *hoxa-4, hoxb-4,* and *hoxd-4* genes show more complete homeotic transformations and a dose-dependent increase in the number of vertebrae transformed. *Genes Dev.* **9**, 1667-1677.

Jeannotte, L., Lemieux, M., Charron, J., Poirier, F. and Robertson, E. J. (1993). Specification of axial identity in the mouse: role of the *Hoxa-5* (*Hox-1.3*) gene. *Genes Dev.* **7**, 2085-2096.

Kostic, D. and Capecchi, M. R. (1994). Targeted disruptions of the murine *hoxa-4* and *hoxa-6* genes result in homeotic transformations of components of the vertebral column. *Mech. Dev.* **46**, 231-247.

LeMouellic, H., Lallemand, Y. and Brûlet, P. (1992). Homeosis in the mouse induced by a null mutation in the *Hox-3.1* gene. *Cell* **69**, 251-264.

Lufkin, T., Dierich, A., LeMeur, M., Mark, M. and Chambon, P. (1991). Disruption of the *Hox-1.6* homeobox gene results in defects in a region corresponding to its rostral domain of expression. *Cell* **66**, 1105-1119.

Manley, N. R. and Capecchi, M. R. (1995). The role of *hoxa-3* in mouse thymus and thyroid development. *Development* **121**, 1989-2003.

Männer, J., Seidl, W. and Steding, G. (1995). The role of extracardiac factors in normal and abnormal development of the chick embryo heart: cranial flexure and ventral thoracic wall. *Anat. Embryol.* **191**, 61-72.

Mansour, S. L., Thomas, K. R. and Capecchi, M. R. (1988). Disruption of the proto-oncogene *int-2* in mouse embryo-derived stem cells: a general strategy for targeting mutations to non-selectable genes. *Nature* **336**, 348-352.

Mansour, S. L., Goddard, J. M. and Capecchi, M. R. (1993). Mice homozygous for a targeted disruption of the proto-oncogene *int-2* have developmental defects in the tail and inner ear. *Development* **117**, 13-28.

Marshall, H., Studer, M., Pöpperl, H., Aparicio, S., Kuroiwa, A., Brenner, S. and Krumlauf, R. (1994). A conserved retinoic acid response element required for early expression of the homeobox gene *Hoxb-1. Nature* **370**, 567-571.

Moebius, P. J. (1888). Uber angeborene doppelseitige Abducens-Facialis Lahmung. *Munch Med. Wochenschr* **35**, 91-94.

Nagy, A., Rossant, J., Nagy, R., Abramow-Newerly, W. and Roder, J. C. (1993). Derivation of completely cell culture-derived mice from early-passage embryonic stem cells. *Proc. Natl. Acad. Sci. USA* **90**, 8424-8428.

Pendleton, J. W., Nagai, B. K., Murtha, M. T. and Ruddle, F. H. (1993). Expansion of the *Hox* gene family and the evolution of chordates. *Proc. Natl. Acad. Sci. USA* **90**, 6300-6304.

Pöpperl, H., Bienz, M., Studer, M., Chan, S.-K., Aparicio, S., Brenner, S., Mann, R. S. and Krumlauf, R. (1995). Segmental expression of *Hoxb-1* is controlled by a highly conserved autoregulatory loop dependent upon *exd/pbx. Cell* **81**, 1031-1042.

Ramirez-Solis, R., Zheng, H., Whiting, J., Krumlauf, R. and Bradley, A. (1993). *Hoxb-4* (*Hox-2.6*) mutant mice show homeotic transformation of a cervical vertebra and defects in the closure of the sternal rudiments. *Cell* **73**, 279-294.

Rancourt, D. E., Tsuzuki, T. and Capecchi, M. R. (1995). Genetic interaction between *hoxb-5* and *hoxb-6* is revealed by nonallelic noncomplementation. *Genes Dev.* **9**, 108-122.

Rijli, F. M., Mark, M., Lakkaraju, S., Dierich, A., Dollé, P. and Chambon, P. (1993). A homeotic transformation is generated in the rostral branchial region of the head by disruption of *Hoxa-2*, which acts as a selector gene. *Cell* **75**, 1333-1349.

Rubock, M. J., Larin, Z., Cook, M., Papalopulu, N., Krumlauf, R. and Lehrach, H. (1990). A yeast artificial chromosome containing the mouse homeobox cluster *Hox-2. Proc. Natl. Acad. Sci. USA* **87**, 4751-4755.

Satokata, I., Benson, G. and Maas, R. (1995). Sexually dimorphic sterility phenotypes in *Hoxa10*-deficient mice. *Nature* **374**, 460-463.

Sham, M. H., Vesque, C., Nonchev, S., Marshall, H., Frain, M., Gupta, R. D., Whiting, J., Wilkinson, D., Charnay, P. and Krumlauf, R. (1993). The zinc finger gene *Krox-20* regulates *HoxB2* (*Hox2.8*) during hindbrain segmentation. *Cell* **72**, 183-196.

Small, K. M. and Potter, S. S. (1993). Homeotic transformations and limb defects in *HoxA-11* mutant mice. *Genes Dev.* **7**, 2318-2328.

Suemori, W., Takahashi, N. and Noguchi, S. (1995). *Hoxc-9* mutant mice show anterior transformation of the vertebrae and malformation of the sternum and ribs. *Mech. Dev.* **51**, 265-273.

Thomas, K. R. and Capecchi, M. R. (1987). Site-directed mutagenesis by gene targeting in mouse embryo-derived stem cells. *Cell* **51**, 503-512.

Thomas, K. R., Deng, C. and Capecchi, M. R. (1992). High-fidelity gene targeting in embryonic stem cells by using sequence replacement vectors. *Mol. Cell. Biol.* **12**, 2919-2923.

van der Hoeven, F., Zakany, J. and Duboule, D. (1996). Gene transpositions in the *HoxD* complex reveal a hierarchy of regulatory controls. *Cell* **85**, 1025-1035.

Waldo, K. L., Kumiski, D. and Kirby, M. L. (1996). Cardiac neural crest is essential for the persistence rather than the formation of an arch artery. *Dev. Dyn.* **205**, 281-292.